OPTIMIZATION OF WELDING PARAMETERS OF Ti6Al4V ALLOY USING ELECTRON BEAM

Petr Havlík[1,*], Ivo Dlouhý[1]

[1] Institute of Materials Science and Engineering, Faculty of Mechanical Engineering, Brno University of Technology, Technická 2, 616 69 Brno, Czech Republic

[*]corresponding author: Tel.: +420 776 247 820, e-mail: havlik03petr@gmail.com

Resume

Titanium alloys and their weld joints find wide application, in particular in the aircraft, automotive and chemical industries, because of their outstanding specific strength and corrosion resistance. The high reactivity of these alloys and the strong degradation effect of elements contained in the atmosphere (H, N and O) make it necessary for these alloys to be welded in protective atmospheres or in vacuum. From this viewpoint, Electron Beam Welding is an advantageous welding technology, especially in large series production. In the literature, there is sufficient information about the effect of the basic welding parameters, namely accelerating voltage, current and welding speed, on the properties of welded joints. In the paper, the effects of the spot diameter and beam focusing on the penetration depth and the weld shape in the Ti6Al4V alloy are studied. The results obtained are complemented by an analysis of the microstructure and microhardness measurements across the welds.

Article info

Article history:
Received 15 March 2016
Accepted 25 April 2016
Online 12 June 2016

Keywords:
Electron beam welding;
Ti6Al4V alloy;
Shape and dimension of weld;
Microstructure;
Hardness.

Available online: http://fstroj.uniza.sk/journal-mi/PDF/2016/02-2016.pdf

ISSN 1335-0803 (print version)
ISSN 1338-6174 (online version)

1. Introduction

Titanium and its alloys are one of the best engineering materials for use in industrial applications [1, 2]. This is due to their properties such as excellent strength-to-density ratio, high fatigue strength, toughness, and good corrosion resistance. These properties make titanium alloys attractive for aerospace applications [3] and also for many chemical, marine, military and sports applications, even though of the price of these alloys is relatively high.

Ti6Al4V alloy is the most widely used titanium alloy, accounting for more than 60 % of the world production of this alloy and serves as the world standard in aerospace applications [4]. At room temperature, this alloy contains the HCP α phase and the BCC β-phase. The mechanical and physical properties of this alloy are controlled by microstructural development during thermo-mechanical processing [5, 6].

At temperatures above 350 °C, particularly in molten state, titanium is very reactive with atmospheric oxygen, nitrogen, hydrogen, and carbon. These interstitial elements reduce ductility and toughness and increase strength and hardness [6]. Contamination by these elements during welding can be caused by poor preparation and cleaning of the joint and filler materials, poor shielding of the weld zone or impurities in the gas.

Titanium may be joined by a variety of conventional fusion welding processes, but its chemical reactivity requires precaution in order to avoid contamination of the fusion and heat-affected zones. Fusion welding of titanium alloy is possible in inert gas shielded arc and high-energy beam welding processes such as Electron

Beam Welding (EBW) and plasma welding [7]. The EBW process is considered superior to others because of the deep and narrow weld zone, reduced heat-affected zone (HAZ) and high reliability. EBW is used relatively often for the welding of Ti alloys, since welding is carried out inside a chamber in which a vacuum is maintained to protect the weld from contamination. Great joint depth, which can be achieved with a high beam power density (1.5×10^4 to 1.5×10^5 $W\cdot mm^{-2}$), and keyhole-mode welding increase the productivity and reduce heat input in comparison to arc-welding processes [8].

The effect of accelerating voltage (U), beam current (I) and welding speed (v) on the depth of penetration and the whole geometry of the weld were studied in [9] for Ti6Al4V alloy via a series of weld trials. The objective of the present study was to optimize the welding parameters of commercial Ti6Al4V alloy by EBW, namely the influence of the spot diameter and the distance of the EB focus from the surface, the size and shape of the weld (weld penetration, the width of the weld metal and HAZ), the microstructure and hardness of individual areas.

2. Experimental material and procedures

The Ti6Al4V alloy was produced by the VSMPO-AVISMA Corporation, Russia. Data on the chemical composition, given in Table I, and results of tensile tests of the alloy in as-supplied condition, that is, annealed at 780°C/1 h/air, have been taken from a copy of the "Inspection Certificate" (see Table 2).

Table 1

Chemical composition (in wt. %) of alloy Ti6Al4V.

Al	V	Fe	O	C	N	H	Ti
6.46	4.11	0.21	0.166	0.007	0.004	0.0055	balance

Table 2

Mechanical properties.

Orientation	Yield strength $R_p0.2$ (MPa)	Tensile strength R_{mT} (MPa)	Elongation A (%)
longitudinal	970-980	1000-1011	14.4-16.0
transverse	985-1010	1020-1040	14.6-15.0

Table 3

Varying parameters of EBW.

Specimen	Beam current I (mA)	Spot diameter (mm)	SURF (mA)
0-1	15 - 20	0.1	- 3
0-2	12 - 17	0.1	- 3
0-3	15 - 20	0.2	- 3
0-4	12 - 17	0.2	- 3
0-5	18	0.3	- 3
0-6	18	0.6	- 3
0-7	18	0.9	- 3
0-8	18	1.2	- 3
0-9	18	0.2	0
0-10	18	0.2	5
0-11	18	0.2	10
0-12	18	0.2	15
0-13	18	0.2	- 5
0-14	18	0.2	- 10
0-15	18	0.2	- 15
0-16	18	0.2	- 20

Material for individual tests was cut from an 8 × 250 × 1000 mm sheet metal plate. Electron beam welding was carried out using an AG&COKGaA device with a K26 industrial welding chamber (a product of the German Probeam company). The parameters of the welds are given in Table 3, together with the designations of individual samples. With all the samples, the welding speed was identical ($20\ mm \cdot s^{-1}$) and so were the accelerating voltage used (120 kV) and the working distance (750 mm). The term spot diameter used in Table 3 corresponds to the diameter of electron beam circular scanning patterns, and the term SURF gives in the given case the values in mA corresponding roughly to the electron beam focusing above (+) and below (–) the surface of individual samples, in mm.

Specimens for the metallographic analysis were ground, polished and etched in Kroll's reagent (2 ml HF, 8 ml HNO_3, 92 ml distilled H_2O). The study of microstructures was carried out using a Zeiss Axio optical microscope and a Zeiss Ultra Plus scanning electron microscope equipped with EDS Oxford analyser.

HV0.1 microhardness tests were conducted using a LECO LM 274AT device.

3. Results and discussion

The microstructure of the Ti6Al4V in as-supplied state (i.e. annealed state) is formed by polygonal grains of the α-phase and, on a much smaller scale, by irregular configurations of the β-phase, which mainly occurs on the α-phase boundaries, as evident in Fig. 1. Part of the α-phase is arranged in lines, with the β-phase occurring inside these grains. The α-phase is assumed to be the result of the transformation of the β-phase, which occurred at an annealing temperature of 780 °C. Via the EDS method it was established that the content of vanadium in the β-phase ranged between 18 and 22 wt. %, which testified to the high value of the coefficient of interphase distribution of vanadium between the two coexisting phases. For the sake of completeness, it should be added that the aluminium content measured in the β-phase is within a narrow range of 2.5 - 4.8 wt. %. In the case of the chemical composition of the α-phase it is quite the contrary (8.6 - 9.6 wt. % Al and 2.8 - 3.3 wt. % V). The state described above is probably a non-equilibrium state.

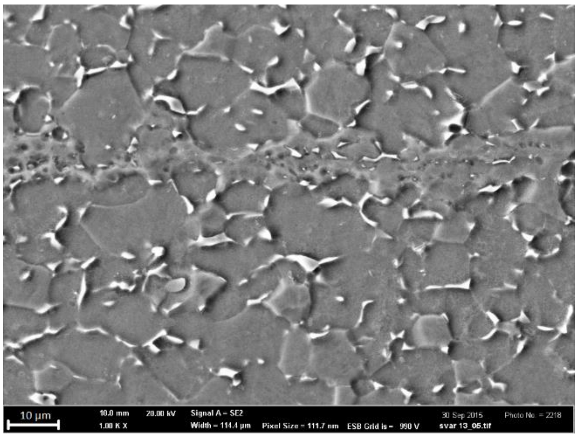

Fig. 1. Microstructure of base material, etch. Kroll, SEM.

One of the pictures of the structure of the welds is given in Fig. 2. Evaluating the structures of all the weld variants given in Table 3 revealed that in the welds there were no discontinuities of the crack and bubble types. The obtained set of pictures of weld structures made it possible to determine the weld depth and the shape and size of the weld metal (WM) and heat-affected zone (HAZ). The shapes and dimensions of the welds are given in Figs. 3 and 4 for individual sizes of the spot diameter, with the beam current, accelerating voltage and welding speed remaining constant. It is obvious from Figs. 3 and 4 that with increasing values of the spot diameter the weld depth decreases markedly while the width of WM (molten pool) increases. The shape and dimensions of the weld, that is, the values of WM and HAZ, also change analogously, with the HAZ width barely changing with the spot diameter value.

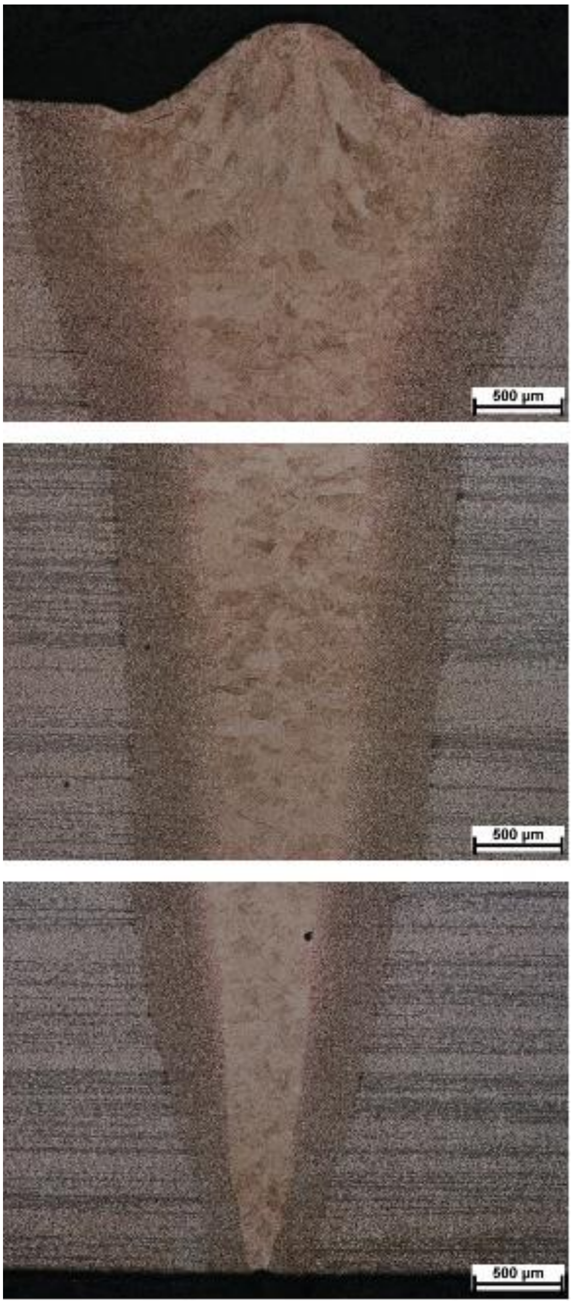

Fig. 2. Macrophotography of EB weld joint.
(full colour version available online)

A simple relation holds for the beam diameter, $d = s\ I/U$, where I is the beam current, U is the accelerating voltage, and s is a constant given by the electron gun optics. Thus in our case the beam diameter was constant. If the beam diameter or the size of spot diameter increases, it can be expected that for a given beam energy given by the $U{\cdot}I$ product the energy will accumulate in a larger volume of material and, consequently, the weld depth will decrease. For a weld depth b, the authors of [9] give the Equation (1)

$$b = C\frac{P}{TD}\sqrt{\frac{K}{vd}} \qquad (1)$$

where C is a constant, P is the beam power, T is the melting point, D is the thermal diffusivity, k is the thermal conductivity and v is welding speed. T, D and k are physical constants so Equation (1) can be rewritten in the form (2)

$$b = CPC_1\sqrt{\frac{1}{vd}} \qquad (2)$$

where $C_1 = \sqrt{K}/TD$ is the material constant. In the given case, the beam diameter in Equation (2) can be replaced by the spot diameter size; then with increasing spot diameter size the weld depth decreases and the weld shape is also changed, as can be seen from Figs. 3 and 4. From the weld shape it can be concluded that for a spot diameter larger than 0.3 mm the mechanism of beam penetration operating in this case is predominantly conduction-mode welding.

The growing value of positive focusing results in an increased diameter of the beam incident on the surface, which, in agreement with Equation (2), leads to decreasing weld depth with increasing distance of focusing of the EB on the surface of the metal sheet (quantified as the “SURF” value); by contrast, the width of WM and HAZ increased on the surface of metal sheet, with the overall shape of the weld remaining almost without change (Fig. 5).

The growing size of negative focusing up to -10 mA led to increasing weld depth; increasing the negative focusing still further had the opposite effect and the weld shapes then corresponded to the removal (predominantly by conduction) of the introduced heat (see Figs. 5 and 6).

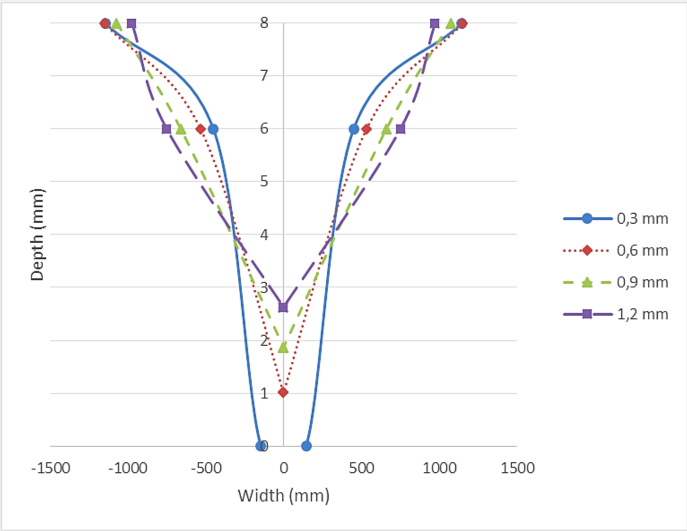

Fig. 3. Influence of the "Spot" on the WM size and shape.
(full colour version available online)

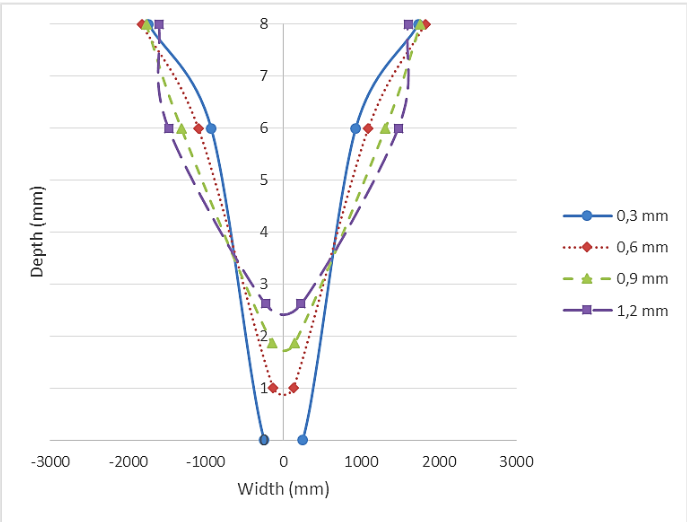

Fig. 4. Influence of the "Spot" on the weld size and shape.
(full colour version available online)

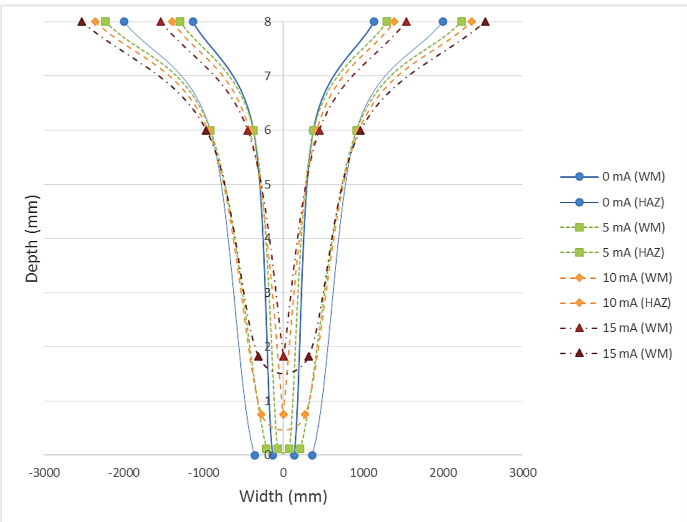

Fig. 5. Shape and dimensions of the welds depending on the size of positive focusing.
(full colour version available online)

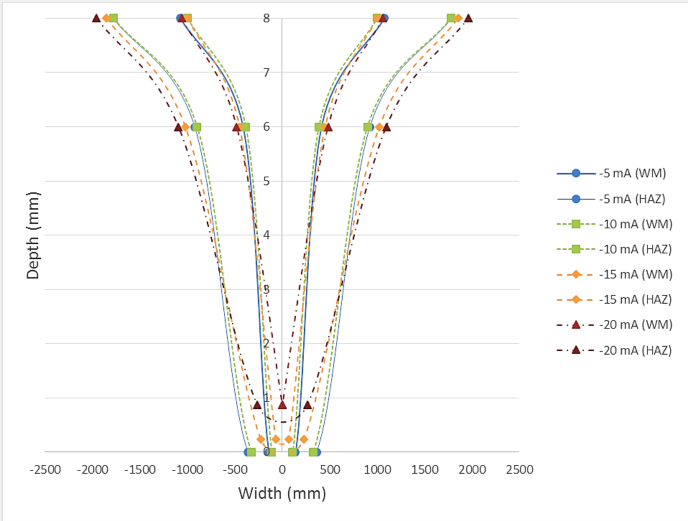

Fig. 6. Shape and dimensions of the welds depending on the size of negative focusing.
(full colour version available online)

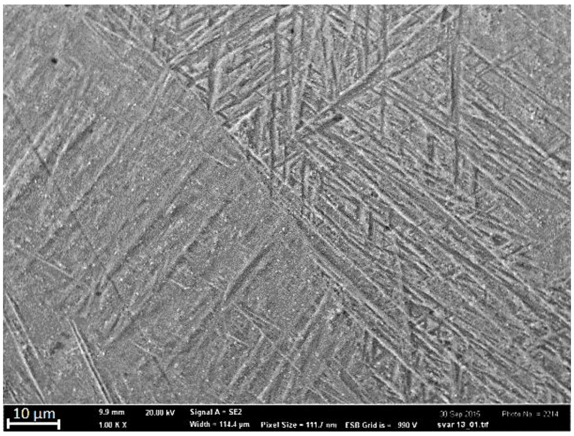

Fig. 7. Microstructure of WM, etch. Kroll, SEM.

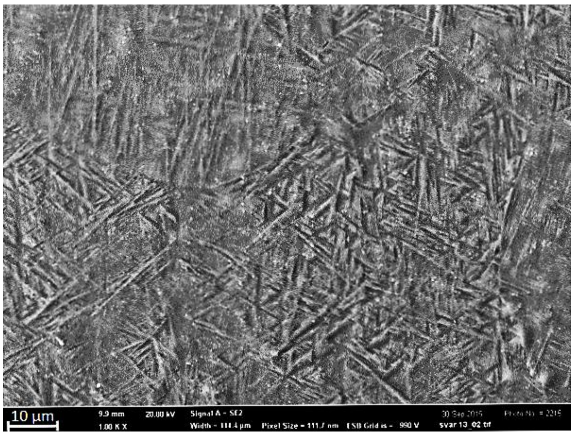

Fig. 8. Microstructure of HAZ (with HAZ followed by WM), etch. Kroll, SEM.

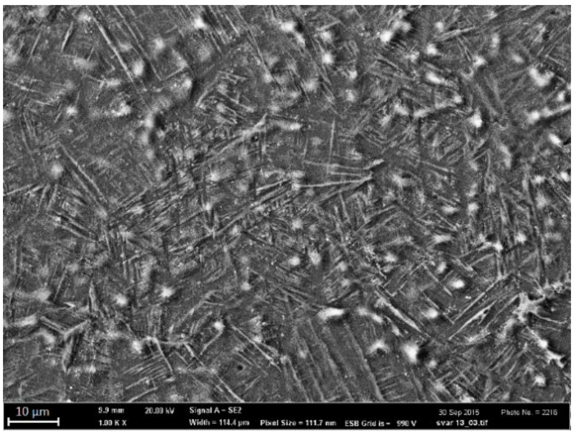

Fig. 9. Microstructure of HAZ (with HAZ followed by BM), etch. Kroll, SEM.

The microstructure of the weld metal is formed by α' martensite and, to a lesser degree, probably also by the β-phase (Fig. 7). The structure of HAZ changes continuously from a predominantly martensitic structure with a major proportion of non-transformed β-phase (Fig. 8) to a structure close to the basic material (Fig. 9). The latter is formed by a mixture of α-phase of acicular and polygonal morphology with the β-phase, whose content is higher when compared with unaffected basic material.

The microstructure analysis was complemented by the measurement of the content of titanium, aluminum and vanadium across the weld interface, using the EDS method, on a line segment 800 μm in length (700 points). The results of this analysis are given in graphical form in Fig. 10. It is evident from this figure that in the course of welding in a vacuum (pressure 3 to 8×10^{-5} mbar) there was no selective evaporation of any of the elements under analysis, which is also attested by the mean concentration values of Ti, Al and V, as calculated for WM and BM (Table 4). It is evident from the standard deviation values, also given in Table 4, that for vanadium they are higher in the case of the BM that in the case of with the WM. This finding is associated with the larger dimensions of the β-phase in the BM and, as mentioned earlier, with the fact that the concentration of vanadium in this phase attains values of up to 22 wt. %.

Table 4

Concentrations in wt. % of Ti, Al and V in weld zones.

Area	Ti	Al	V
WM	90.0±1.0	5.7±0.5	4.3±0.9
BM	90.1±1.5	5.7±0.6	4.2±1.5

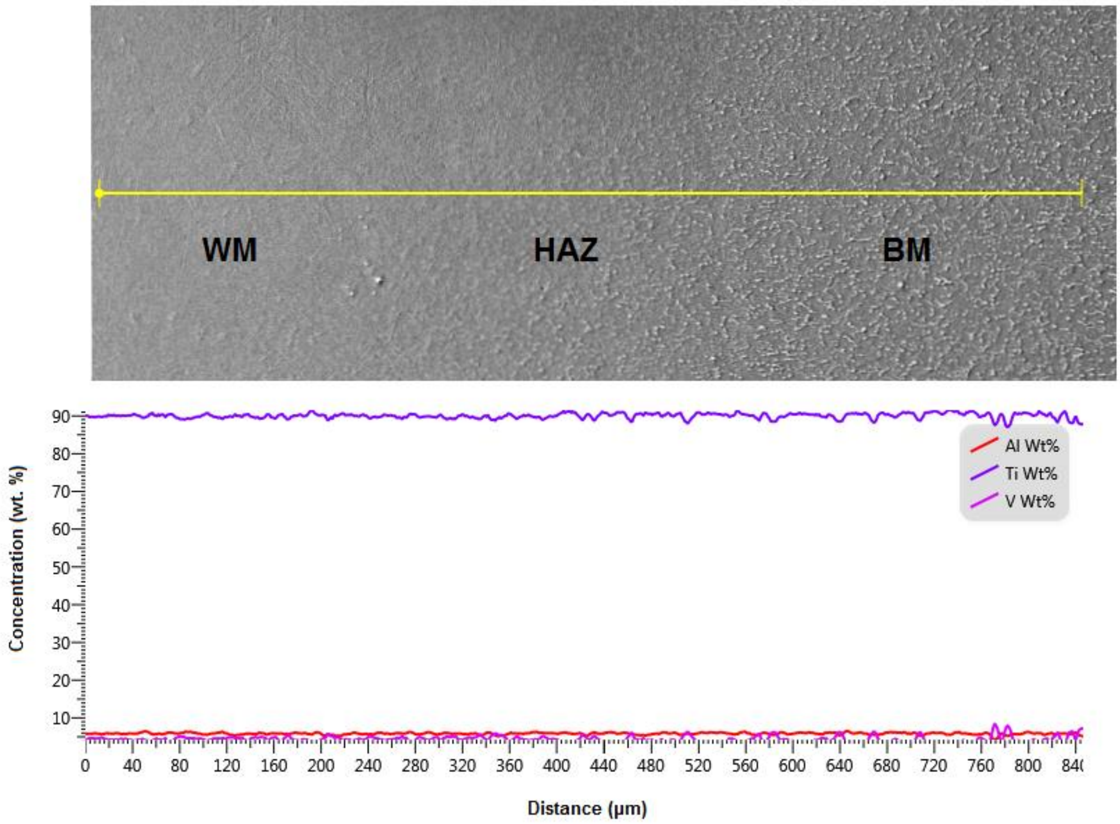

Fig. 10. Concentration distribution of Ti, Al and V across the weld.
(full colour version available online)

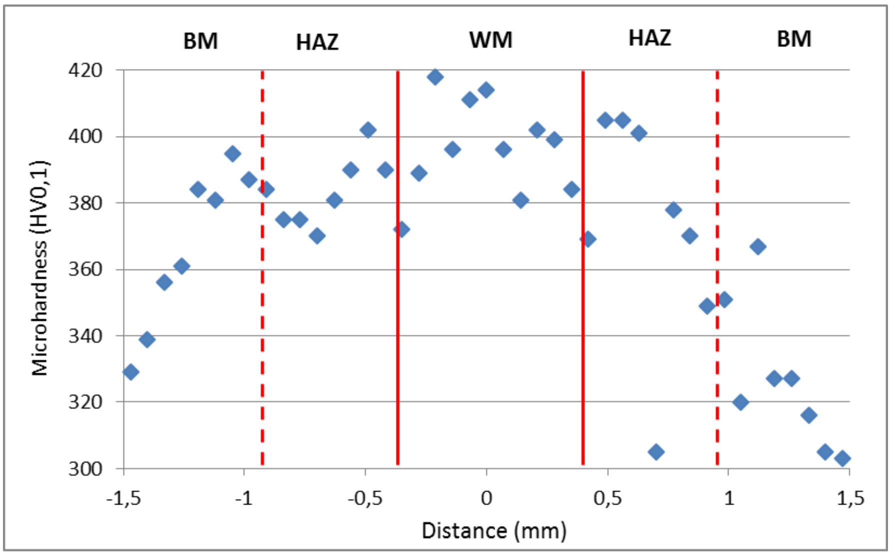

Fig. 11. Microhardness HV0.1 across the weld, spec. 14.
(full colour version available online)

An example of the development of HV0.1 microhardness values across the weld of sample 14 can be seen in Fig. 11. The values of 380 - 420 HV0.1 correspond to the martensitic structure of WM in the whole set of samples; the same values were measured by the authors of [9]. Laboratory heat treatment - quenching at 1035 °C/10 min/water - led to the value of 390 HV1 with predominantly martensitic structure while the heat treatment mode 1035 °C/10 min/water with predominantly acicular and less frequently Widmannstätten morphology of the α-phase led to the value of 320 HV1, with a BM hardness of 330 HV0.1. The HV values under different loading are not fully comparable but it can be said that substantial differences in the microstructure correspond with pronounced changes in hardness values. In the welds examined, the differences in values between WM and BM amounted to as much as 70 HV0.1. The same differences were observed by the authors of [10], who additionally compared the results of tensile tests and impact bending tests on samples taken from BM and EBW. In the case of EBW the fracture surfaces were in the WM. It follows from the above comparison that the yield point values (960 MPa) and tensile strength values (1000 MPa) do not change but in WM there were drops in the values of elongation (12.7 → 7.7 %), contraction (34.3 → 21.0 %) and impact energy (16 → 10 J). The weld joint is thus considerably more brittle and must therefore be annealed.

4. Conclusions

The effects of spot diameter in the range of 0.3 - 1.2 mm and focusing in the interval of -20 to +15 mA, on the penetration depth and weld shape in Ti6Al4V alloy were studied under constant values of the beam current I (18 mA), accelerating voltage U (120 kV) and welding speed v (20 $mm \cdot s^{-1}$). The study yielded the following knowledge:

- Increasing the size of the spot diameter has the same effect on the weld depth as the beam diameter, that is, with increasing spot diameter the depth of the weld decreases and the weld width increases, particularly in the weld face area.
- Positive focusing of the electron beam has an analogous effect on the weld depth to increases in the spot diameter value.
- Increasing the negative focusing to -10 mA led to increased weld depth; increasing the negative focusing still further had the opposite effect.

- The conditions in which the welds were produced probably did not lead to selective evaporation of the alloy elements (verified for a spot diameter of 0.2 mm and focusing of -10 mA).
- The marked differences in the hardness values of WM (400 HV0.1) and BM (335 HV0.1) indicate the necessity of post-weld heat treatment of real welds.
- For the 8 mm thick metal sheet and the I, U and v values used, the spot diameter should range between 0.3 and 0.6 mm with focusing at -3 mA, while focusing should acquire values of +5 mA (too wide a weld) and -5 mA (to be preferred).

Acknowledgements

This work has been supported by European Regional Development Fund in the framework of the research project NETME Centre under the Operational Program Research and Development for Innovation No. CZ.1.5/2.1.00/01.002 and within the project NETME plus (Lo1202), project of Ministry of Education, Youth and Sports, under the "national sustainability programme".

References

[1] R.R. Boyer, G. Welsch, E.W. Collings, eds.: Materials properties handbook: Titanium and titanium alloys, ASM International, Materials Park, OH 1994.

[2] M.J. Donachie: Titanium: A Technical Guide, 2nd edition, ASM International, Materials Park, OH 2000.

[3] R.R. Boyer: Mater. Sci. and Eng. A213 (1996) 103-114.

[4] J.L. Barreda, F. Santamaria, X. Azpiroz, A. M. Irisarri and J. M.. Varona: Vacuum 62(2-3) (2001) 143-150.

[5] S. Banerjee, P. Mukhopadhyay: Phase Transformation, Examples from Titanium and Zirkonium Alloys, Elsevier 2007.

[6] G. Lütjering: Mater. Sci. Eng. A243 (1998) 32-45.

[7] Li, Leijun et al. eds.: ASM Handbook: Welding Fundamentals and Processes, Vol. 6A. ASM International, Materials Park, OH 2011.

[8] H. Schultz: In: Electron Beam Welding, Woodhead Publishing Ltd. 1994.

[9] T.S. Balasubramanian, M. Balakrishnan, V. Balasubramanian, M.A. Muthu Manickam: STWJ 16(8) (2011) 702-708.

[10] G. Thomas, V. Ramachandra, K. V. Nagarajan, B. Pant, B. K. Sarkar and R. Vasudevan: In: Welding Research Supplement, 1989, pp. 336-341.